ORIGINAL ARTICLE

Performance evaluation of real-time global ionospheric maps provided by different IGS analysis centers

Xiaodong Ren[1,2] · Jun Chen[1,3] · Xingxing Li[1] · Xiaohong Zhang[1,3,4] · Mohamed Freeshah[4,5]

Abstract

With the development of real-time precise clock and orbit products, high-precision real-time ionospheric products have become one of the most critical resources for real-time single-frequency precise point positioning. Fortunately, there are several international GNSS service (IGS) analysis centers, e.g., UPC, WHU, and CAS, that are providing real-time global ionospheric maps (RT-GIMs). We evaluate these maps in detail over 2 years for different aspects. First, the RT-GIMs and 1-day predicted ionospheric products (C1PG GIM) differenced with the IGS final GIMs (IGSG GIM) are performed. Second, ionospheric vertical total electron content from Jason-2/3 data is set as a reference to evaluate the quality of RT-GIMs over oceanic regions. Third, 22 stations, which are not used in the generation of RT-GIMs, C1PG GIM, and IGSG GIM, are selected and the difference of slant total electron content (dSTEC) method is used to assess the accuracy and consistency of RT-GIMs over continental regions. Finally, the performance of RT-GIMs in the position domain is demonstrated based on SF-PPP solutions. The results show that the accuracy of the RT-GIMs is slightly worse than that of C1PG GIM and IGSG GIM. All RT-GIMs and the C1PG GIM have a smaller mean difference compared to the IGSG GIM by (−0.97, −0.90, −0.77, −0.80) TECU for (UPC RT-GIM, CAS RT-GIM, WHU RT-GIM, C1PG GIM). Over oceanic regions, the RT-GIMs perform nearly the same as the C1PG GIM, but a slightly worse than IGSG GIM. The STDs are (3.96, 3.05, 3.25, 3.12, 2.54) TECU relative to Jason-2 and (4.94, 3.24, 3.38, 3.24, 2.65) TECU relative to Jason-3 for (UPC RT-GIM, CAS RT-GIM, WHU RT-GIM, C1PG GIM, IGSG GIM), respectively. Comparing with dSTEC values observed from the selected ground stations over continental regions, the RMS is (4.02, 2.16, 2.29, 1.86, 1.49) TECU for (UPC RT-GIM, CAS RT-GIM, WHU RT-GIM, C1PG GIM, IGSG GIM). In the position domain, the positioning accuracy of SF-PPP solution corrected by the RT-GIMs and C1PG GIM can reach decimeter level in the horizontal direction and meter level in the vertical direction, which is worse than obtained by IGSG GIM. Meanwhile, the positioning accuracy of SF-PPP corrected by RT-GIMs is almost the same as that obtained using C1PG GIM. For RT-GIMs, the accuracy of the CAS RT-GIM is slightly better than that of the other two RT-GIMs.

Keywords Real-time global ionosphere maps (RT-GIMs) · Ionospheric products · Single-frequency precise point positioning (SF-PPP) · Global navigation satellite system (GNSS) · IGS associate analysis centers (IAACs)

✉ Xiaodong Ren
  renxiaodongfly@gmail.com

✉ Xiaohong Zhang
  xhzhang@sgg.whu.edu.cn

[1] School of Geodesy and Geomatics, Wuhan University, 129 Luoyu Road, Wuhan 430079, China

[2] Deutsches Geodätisches Forschungsinstitut der Technischen Universität München (DGFI-TUM), Arcisstraße 21, 80333 Munich, Germany

[3] Key Laboratory of Geospace Environment and Geodesy, Ministry of Education, 129 Luoyu Road, Wuhan 430079, China

[4] Collaborative Innovation Center for Geospatial Technology, 129 Luoyu Road, Wuhan 430079, China

[5] State Key Laboratory of Information Engineering in Surveying, Mapping and Remote Sensing, Wuhan University, Wuhan 430079, China

Introduction

Due to the dispersive characteristic of the ionosphere, dual- or multi-frequency GNSS users can eliminate the first-order ionospheric delays using ionospheric-free (IF) combination observations. Single-frequency GNSS users can mitigate the ionospheric delays by the IF combination of code and phase measurements known as GRoup And PHase Ionospheric Correction (GRAPHIC) (Yunck 1993; Choy 2009) or estimate it as one of the unknown parameters simultaneously along with other parameters. However, the performance of SF-PPP corrected by this approach suffers from long convergence time. Another important method is that of using ionosphere models, e.g., the Klobuchar model (Klobuchar 1987) and its refined models (Yuan et al. 2008; Bi et al. 2017; Chen et al. 2017), the NeQuick model (Nava et al. 2008; Brunini et al. 2011a, b; Angrisano et al. 2013), the NTCM model (Hoque and Jakowski 2015, 2018) and its modification MNTCM-BC (Zhang et al. 2017), or the BDS broadcast model (BDGIM) and its improvements (Wang et al. 2018, 2019; Yunbin et al. 2019). However, the accuracy of the broadcast ionospheric models is low. Compared to the broadcast ionospheric models, the final global ionospheric maps (GIMs) provided by the associate analysis centers (IAACs) of the International GNSS service (IGS) have a higher accuracy of 2–8 TECU (total electron content unit), which corresponds to an improvement of more than 50% (Orús et al. 2002). However, this type of final GIMs cannot be used for real-time SF-PPP (RT SF-PPP) due to the significant latencies of 1–14 days (Hernández-Pajares et al. 2009; Roma-Dollase et al. 2018).

At present, the IGS is providing different kinds of real-time precise orbit and clock products for real-time PPP (RT-PPP). This real-time orbit and clock products can achieve the accuracy of 3–5 cm and 0.1–0.15 ns, respectively, which make allows real-time dual-frequency PPP (RT DF-PPP) at the centimeter to decimeter level (Hadas and Bosy 2015; Kazmierski et al. 2017; Zhang et al. 2018). However, the positioning accuracy of RT SF-PPP, as well as the convergence time of RT, highly depends on

the ionospheric delay corrections. At present, the three IAACs, i.e., Universitat Politècnica de Catalunya (UPC), Wuhan University (WHU), and the Chinese Academy of Sciences (CAS), are computing, in an experimental way, real-time GIMs (RT-GIMs) products made available to users through FTP or internet protocol (Ntrip). Several studies have been conducted to assess the IGS final, rapid and predicted GIM products as well as the CNES RT-GIMs product (Hernández-Pajares et al. 2017; Roma-Dollase et al. 2018; Li et al. 2018a, b; Nie et al. 2019). However, an update of the first assessment of RT-GIMs (Roma et al. 2016), which includes the three IAACs RT-GIMs products, is not yet available.

We evaluate the quality of these three RT-GIMs in detail from different aspects, and we also compare them with the predicted ionospheric products of 1-day vertical total electron content (VTEC) maps provided by Center for Orbit Determination (CODE) (C1PG GIM) and to IGS final ionospheric products (IGSG GIM). A brief introduction of the real-time products is presented first. Afterward, their performance is evaluated regarding the following aspects: (1) comparison with IGSG final GIM, (2) direct validation against VTEC altimeter, (3) self-consistency analysis using the difference of slant total electron content (dSTEC) technique based on GNSS phase observations only, (4) positioning accuracy analysis of RT SF-PPP corrected with different RT-GIMs. Finally, summaries and conclusions are presented.

Comparison of ionospheric modeling strategies for three IAACs RT-GIMs

Table 1 lists some information for the three RT-GIMs provided by the various IAACs. As we can see, they use their own software to produce corresponding RT-GIM products. Both WHU and CAS use spherical harmonics function, while UPC adopts the dual-layer-voxel-based tomographic and kriging model introduced in Orús et al. (2005) for post-processed GIMs. Also, WHU and CAS use GNSS observation for modeling the ionosphere and update every 5 min, while UPC models the ionosphere with GPS observation only and updates every

Table 1 Comparison of the modeling strategies for RT-GIMs

Item	WHU	CAS	UPC
Software	GNSS IRIS	GIM_AOE	RT-TOMION-GIM-v0
Fitting function	Spherical harmonics	Spherical harmonics	Tomographic with kriging
ID	rt_ whug	rt_casg	urtg
Observation	GNSS	GNSS	GPS
Maps interval	5 min	5 min	15 min
Spatial resolution	5°×2.5°	5°×2.5°	5°×2.5°
Format	Ionex	Ionex	Ionex
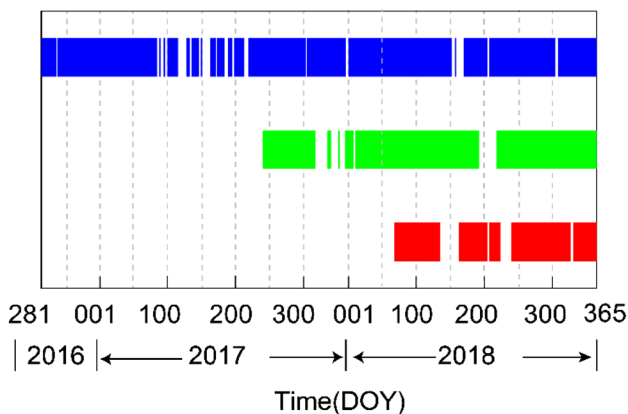
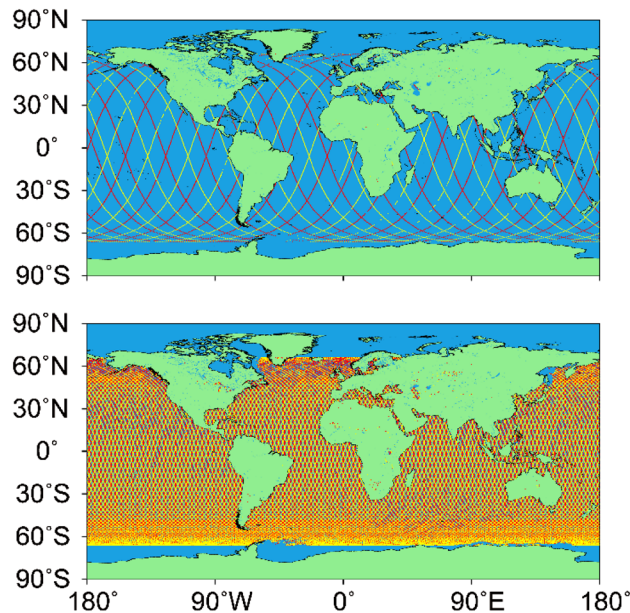Fig. 1 Availability of RT-GIM products provided by UPC (blue), CAS (green), and WHU (red)

Fig. 2 Paths of Jason-2/3 on DOY 001, 2017 (top), and covering during repeat cycle (bottom). Red lines denote Jason-2; yellow lines denote Jason-3

15 min. The spatial resolution of all RT-GIMs is 5° and 2.5° in longitude and latitude, respectively.

Figure 1 depicts the availability of RT-GIM products by individual IAACs. As shown, the period of these RT-GIM products covers about 2 years and 3 months for UPC, a year and a half for CAS, and 9 months for WHU. There are several gaps during the period of products delivery, during which the products are not available. These gaps may occur because the service is still young, the processing software is still subject of improvement, and the real-time data are not stable yet.

VTEC-altimeter assessment method

The direct VTEC data, which are independent of GNSS-based VTEC, can be obtained from the onboard dual-frequency altimeters of the Jason-2 and Jason-3 satellite. Note that the Jason measurements have an offset of a few TECU compared to GNSS-based GIMs (Jee et al. 2010). However, as is shown in Fig. 2a, b, the Jason-2/3 satellites move from about 65°S to 65°N and cover nearly all the oceanic regions except for high-latitude regions. In this sense, it is an excellent choice to assess the GNSS-based vertical TEC ionospheric models over the ocean, i.e., in challenging conditions due to the typical large distances to the stations contributing to the RT-GIM. Generally, the onboard altimeter observations contain two frequencies, i.e., a Ku-band (13.575 GHz) as main frequency and a C-band (5.3 GHz) as auxiliary frequency. The Jason-2/3 VTEC data are derived from the vertical phase ionospheric delay provided in Ku-band frequency as shown:

$$\text{VTEC} = -\frac{dR \cdot f_{\text{Ku}}^2}{40.3} \tag{1}$$

where dR is Ku-band ionospheric range correction and f_{Ku} is Ku-band frequency in GHz. In this study, we use a 21-s

smoothing window to reduce the inherent noise effects of the altimeter (Imel 1994).

Also, the VTEC values extracted from RT-GIMs are calculated by linear interpolation for the corresponding time and location of the altimetry observations. Furthermore, the local time-like based interpolation procedure given in Schaer et al. (1998) is performed in the sun-fixed coordinate system between consecutive epochs.

Self-consistency assessment method based on GNSS measurements

The ionospheric information obtained from GNSS dual-frequency measurements can be used to assess the self-consistency of GNSS-based ionospheric models over continents and in slant line-of-sight directions. Currently, there are two ways to extract ionospheric information for evaluating ionospheric models. One is slant total electron content (STEC) obtained from geometry-free linear combinations of pseudorange and carrier phase measurements based on carrier-to-code leveling (CCL) approach (Komjathy 1997; Mannucci et al. 1998). The other one is dSTEC directly calculated with carrier phase measurements only (Feltens et al. 2011). Since the original STEC measurements based on CCL approach contain receiver- and satellite-differential code bias (DCBs) (Ciraolo et al. 2007; Wang et al. 2016; Li et al. 2018a, b), it is necessary to remove this type of bias through DCB products provided by IAACs (Keshin 2012). It should be noted that the derived STEC in this

approach suffers significantly from the leveling errors of CCL and the correction errors of DCBs. Some studies have shown that the precision of the derived STEC for low geomagnetic regions is about 2 and 10 TECU during low and high solar activity, respectively (Brunini and Azpilicueta 2010).

Due to lower noise and multi-path effects for carrier phase, dSTEC retrieved from the difference of carrier phase provides an exact reference measurement to validate ionospheric models (Hernández-Pajares et al. 2017). In general, dSTEC is defined as the difference between STEC at each epoch along a phase-continuous arc and STEC at the highest elevation in the same arc. Some studies show that the accuracy of directly observed dSTEC is better than 0.1 TECU and there are no assumptions or model errors (Feltens et al. 2011; Hernández-Pajares et al. 2017). Therefore, we adopt the dSTEC assessment method to evaluate the self-consistency and accuracy of different RT-GIMs.

The principle schematic drawing of this method is shown in Fig. 3, which mainly comprises three steps as follows. First, calculate ionospheric data based on GNSS phase observations from selected ground stations at each epoch in a phase-continuous arc:

$$L_4 = L_1 - L_2 = -\gamma \cdot \frac{f_1^2}{40.3 \times 10^{16}} \cdot STEC_{L_4}$$
$$+ \lambda_1 \cdot N_1 - \lambda_2 \cdot N_2 + c \cdot b_r - c \cdot b^s + \varepsilon + \xi \qquad (2)$$

where L_1 and L_2 are GNSS carrier phase observations in length units at frequency f_1 and f_2, respectively; L_4 denotes geometry-free combination of dual-frequency carrier phase observations; N is phase integer ambiguity; $STEC_{L_4}$ repre-

sents STEC along the line of sight (LoS); γ denotes scale factor, which can be calculated by $\gamma = 1 - f_1^2/f_2^2$; λ refers to the wavelength of GNSS signal; c is speed of light; b_r and b^s represent hardware delays of carrier phase at the receiver and satellite side, respectively; ε denotes noise error and multi-path effects; ξ expresses the other kinds of error, e.g., windup term.

Second, search for the observing epoch with the highest satellite elevation in the phase-continuous arc and set the corresponding STEC value as a reference value to calculate dSTEC for each epoch, which can be described as:

$$dSTEC_{L_4}(t) = STEC_{L_4}(t) - STEC_{E\max}$$
$$= \frac{40.3 \times 10^{16}}{f_1^2} \cdot \frac{1}{\gamma} \cdot (L_4(t) - L_{4,E\max}) \qquad (3)$$

where $dSTEC_{L_4}(t)$ denotes dSTEC value obtained from carrier phase at epoch t in the continues arc; $STEC_{E\max}$ represents STEC value extracted from the LoS with highest elevation $E_{\max}$ of the arc; $L_{4,E\max}$ is geometry-free combination of dual-frequency carrier phase observations on $E_{\max}$ of the arc; the meaning of the other parameters in (3) is the same as that in (2).

Finally, calculate the corresponding $dSTEC_{GIM}(t)$ values from GIMs in the same phase-continuous arc of $dSTEC_{L_4}(t)$. Since TEC values provided by IGS GIMs are VTEC with a temporal resolution (e.g., 5 min, 2 h) and spatial resolution (e.g., $2.5° \times 5°$), it is necessary to interpolate the VTEC at the corresponding epoch and convert VTEC into STEC using the modified single-layer mapping function (Schaer 1999).

SF-PPP assessment method

It is known that ionospheric delay is one of the major error sources in single-frequency GNSS positioning. If the other error corrections for SF-PPP solution are the same, the positioning performance highly depends on the ionospheric correction. For this reason, SF-PPP is an appropriate way to perform the quality of RT-GIMs. In this study, the SF-PPP processing strategies are summarized in Table 2.

Results and discussion

We begin with the comparison to IGS GIM. Then, the Jason-2/3 VTEC data are used to evaluate the vertical accuracy of the three RT-GIMs, C1PG GIM, and IGSG GIM over the oceanic region. The dSTEC assessment method is adopted to analyze the self-consistency of these five GIMs in slant line-of-sight directions. At last, we used SF-PPP technique
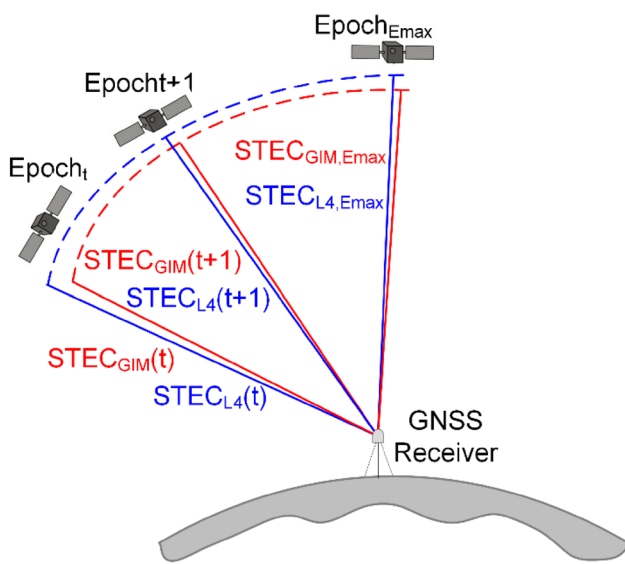

Fig. 3 Principle schematic drawing of dSTEC assessment method

Table 2 Details processing strategies for SF-PPP solution

Item	Processing strategies
Observations	Observation from GPS
Positioning mode	Kinematic
Sampling rate	30 s
Elevation cutoff angle	15°
Satellite orbit	Orbit products from GFZ
Satellite clock	Clock products from GFZ
Zenith tropospheric delay	Initial model + random walk model
Tropospheric gradients	Random walk model
Tropospheric mapping function	Global Mapping Function (GMF)
Phase-windup effect	Corrected
Receiver clock	Estimated, white noise
Satellite antenna phase center	Corrected
Receiver antenna phase center	Corrected
Ionospheric delay	Different ionospheric products
Ionospheric mapping function	Modified single-layer mapping function

to test the performance of SF-PPP solutions corrected by different GIMs.

Comparison to IGS final GIM products

Currently, the IGSG GIM is one of the best ionospheric products having high accuracy and reliable quality (Feltens 2003); it is generated by the combination of four final GIMs products provided by CODE, UPC, European Space Agency (ESA), and Jet Propulsion Laboratory (JPL). In this section, we select IGSG GIM as a reference value to determine the accuracy of the three RT-GIM products. On the other side, the predicted ionospheric products constitute currently one of the essential ionospheric delay corrections for RT SF-PPP users. Therefore, we also present the performance of the difference between the three RT-GIM products and the predicted ionospheric products. Moreover, the performance of various IGS predicted GIMs has been documented in previous studies (García-Rigo et al. 2011; Li et al. 2018a, b), and the C1PG GIM provided by CODE is only adopted in this study.

Figure 4 presents the differences between for the RT-GIMs and C1PG GIM, relative to IGSG GIM on DOY 121, 2018. As shown, in general, the differences between the GIMs show a similar variation trend in that maximum values mainly occurs at low latitudes, especially over the equatorial ionization anomaly (EIA) regions (Davies 1990). The mean deviation for UPC RT-GIM, CAS RT-GIM, WHU RT-GIM, and C1PG GIM on this day is −0.58, −0.08, −0.63 and 0.10 TECU, respectively, which is related to the to the estimation strategy of IGS final GIM leading to a higher VTEC value compared with other kinds of final GIMs (Ren et al. 2016). However, the three RT-GIMs show a different performance; in particular, the deviation of UPC RT-GIM is larger than the other two RT-GIMs, and the most significant difference for UPC compared to IGSG GIM can reach about 10–20 TECU over some regions. This is not the case when the UPC RT-GIM is computed in spherical harmonics and provided in RTCM format, showing a performance comparable to the other two IGS RT-GIMs and working as well in RT (CNES and CAS), when they are compared to JASON-3 VTEC measurements (Hernández-Pajares 2019). Also, the
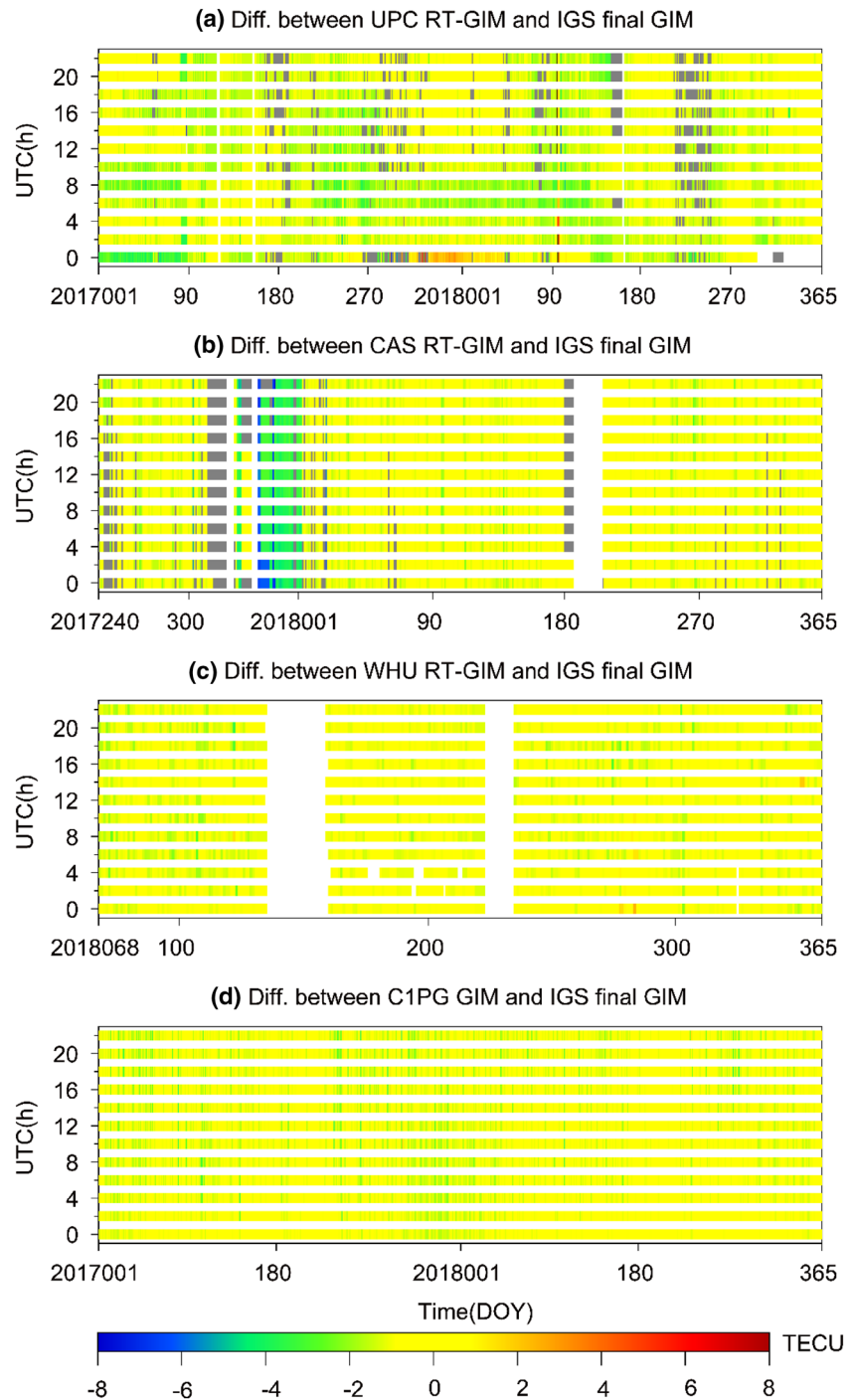

Fig. 4 Differences between the three RT-GIMs and C1PG GIM compared to IGSG GIM at DOY 121, 2018. The top row to bottom rows refer to 0:00 UTC, 6:00 UTC, 12:00 UTC, and 18:00 UTC, respectively. The gray parts denote grid points for which VTEC is not available
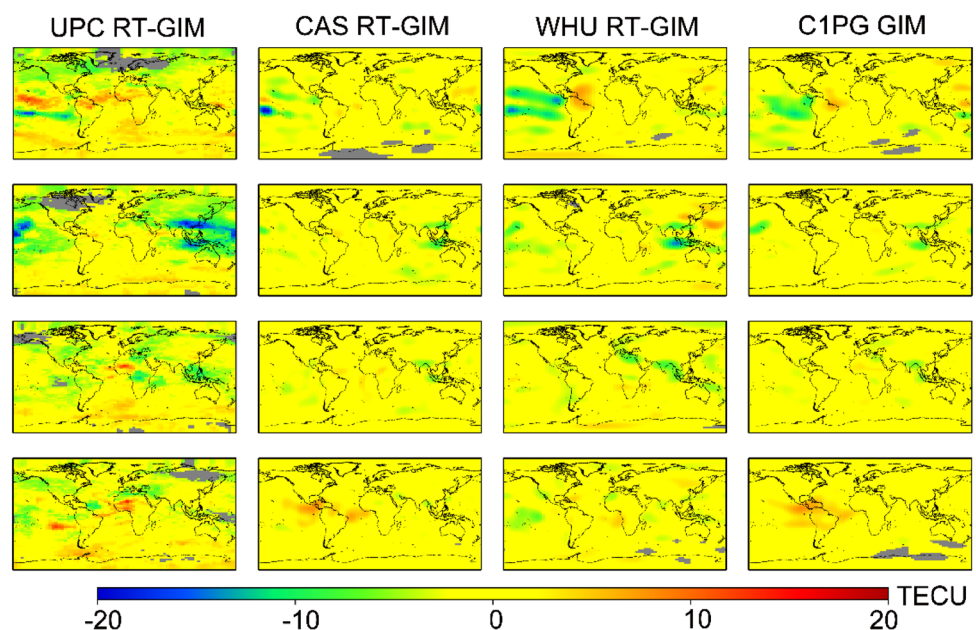
number of unavailable grids for UPC RT-GIM is higher than for the other two RT-GIMs, which is likely associated with fewer receivers; the distribution of the unavailable grids is mainly located in high-latitude areas. On the other hand, the results of CAS RT-GIM over the oceanic region show a better performance than the other two RT-GIMs, but it is worse than C1PG GIM.

To further understand the performance of different RT-GIMs over a long time, we show the differences of them every 2 h during for all available days in Fig. 5. Again, the gray parts denote that the provided data are not available at the corresponding epoch and the blank parts mean the GIMs did not provide the data at the corresponding epoch. We can see that the mean differences of UPC RT-GIM relative to IGSG GIM range from −4 to 0 TECU while its

Fig. 5 Variation of the differences between the three RT-GIMs and C1PG GIM compared to IGSG GIM every 2 h during their available days
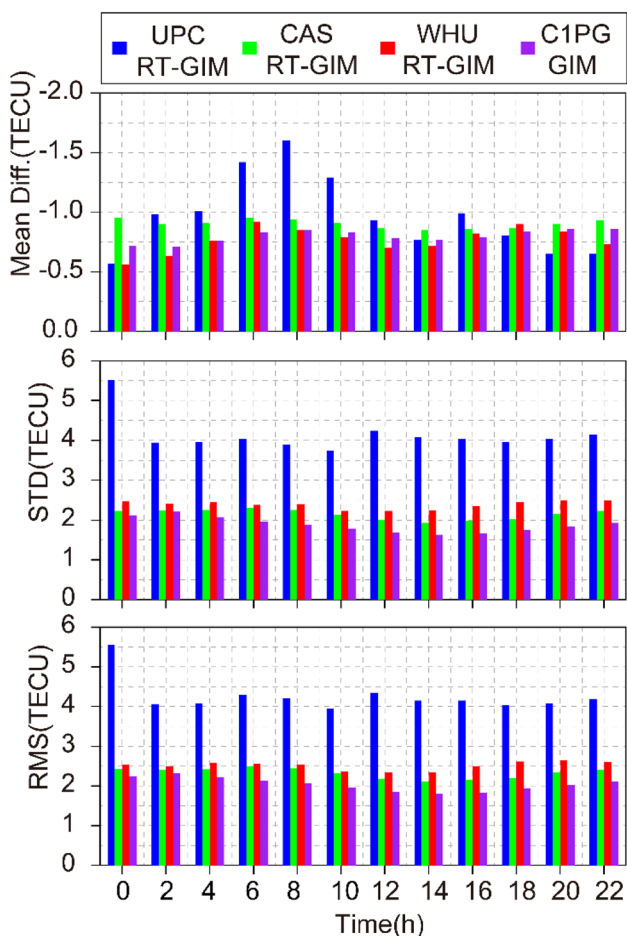
Fig. 6 Mean difference between the three RT-GIMs, C1PG GIM, and IGSG GIM every 2-h products for their available days

absolute difference of some epochs can be larger than 4 TECU. For the CAS RT-GIM, WHU RT-GIM, and C1PG GIM, the mean differences range from − 2 to 2 TECU. It is worth noting that the accuracy and stability of CAS RT-GIM improve significantly after DOY 365, 2017. From the statistical result, as shown in Fig. 6, we can see that STD and RMS of CAS and WHU RT-GIM, which are about 2.0 to 2.5 TECU for each compared epoch, are slightly larger than for C1PG GIM. However, the performance of UPC RT-GIM is worse than C1PG GIM, and the difference is mainly

about 4.0 TECU. Moreover, the statistical results during the experimental time period (without parenthesis) and the common time period for the three RT-GIMs (with parenthesis) are summarized in Table 3. It shows that RT-GIMs have a good agreement with C1PG GIM except for UPC RT-GIM, which is caused by the same spherical function used by the RT-GIM from CAS, WHU, and C1PG. For different RT-GIMs, CAS RT-GIM is the best, and WHU RT-GIM performs better than UPC RT-GIM.

Validation against Jason-2/3 VTEC

To perform a comprehensive comparison and evaluate the performance of the three RT-GIMs over the oceanic region, we calculate the time series of bias, STD and RMS between GIM VTEC and Jason-2 VTEC, and Jason-3 VTEC from DOY 001, 2017, to DOY 360, 2018, which are shown in Fig. 7. The experimental time period covers most of UPC RT-GIM and the beginning days of CAS RT-GIM and WHU RT-GIM. All GIMs show a good agreement for the test period. The daily mean biases of RT-GIMs are mainly between 0 and 4 TECU for Jason-2 VTEC and between 3 and 6 TECU for Jason-3 VTEC. The daily averaged biases of C1PG GIM and IGSG GIM are mainly of 1–4 TECU for Jason-2 VTEC and 4–6 TECU for Jason-3 VTEC. Furthermore, the accuracy of the RT-GIMs is slightly worse than that for C1PG GIM and IGSG GIM, which STD and RMS are mainly ranging from 3 to 6 TECU and 2–6 TECU for Jason-2 VTEC and Jason-3 VTEC, respectively. To compare the statistical results of different GIMs, we calculate the mean bias, STD, and RMS for the test period. Table 4 gives the results during the experimental time period (without parentheses), and the common time period for the three RT-GIMs (with parentheses). It shows that CAS RT-GIM matches with Jason-2/3 VTEC data better than WHU RT-GIM and UPC RT-GIM. Also, the performance of the three RT-GIMs is nearly the same as that of C1PG GIM over the oceanic region.

The distribution of bias values between different the GIMs and Jason-2/3 VTEC data is presented in Figs. 8 and 9. The gray squares indicate no Jason-2/3 VTEC values are

Table 3 Mean difference, STD, and RMS for the GIMs during the experimental time period (without parentheses) and the common time period for the three RT-GIMs (with parentheses). Unit: TECU

Item	UPC RT-GIM	CAS RT-GIM	WHU RT-GIM	C1PG GIM
Mean difference	−0.97 (−1.14)	−0.90 (−0.73)	−0.77 (−0.77)	−0.80 (−0.73)
STD	4.13 (3.27)	2.14 (1.47)	2.38 (2.38)	1.88 (1.52)
RMS	4.26 (3.70)	2.33 (1.67)	2.51 (2.51)	2.04 (1.73)

Fig. 7 Time series of the bias, STD, and RMS of the five GIM products relative to Jason-2/3 VTEC data from DOY 001, 2017 to DOY 360, 2018
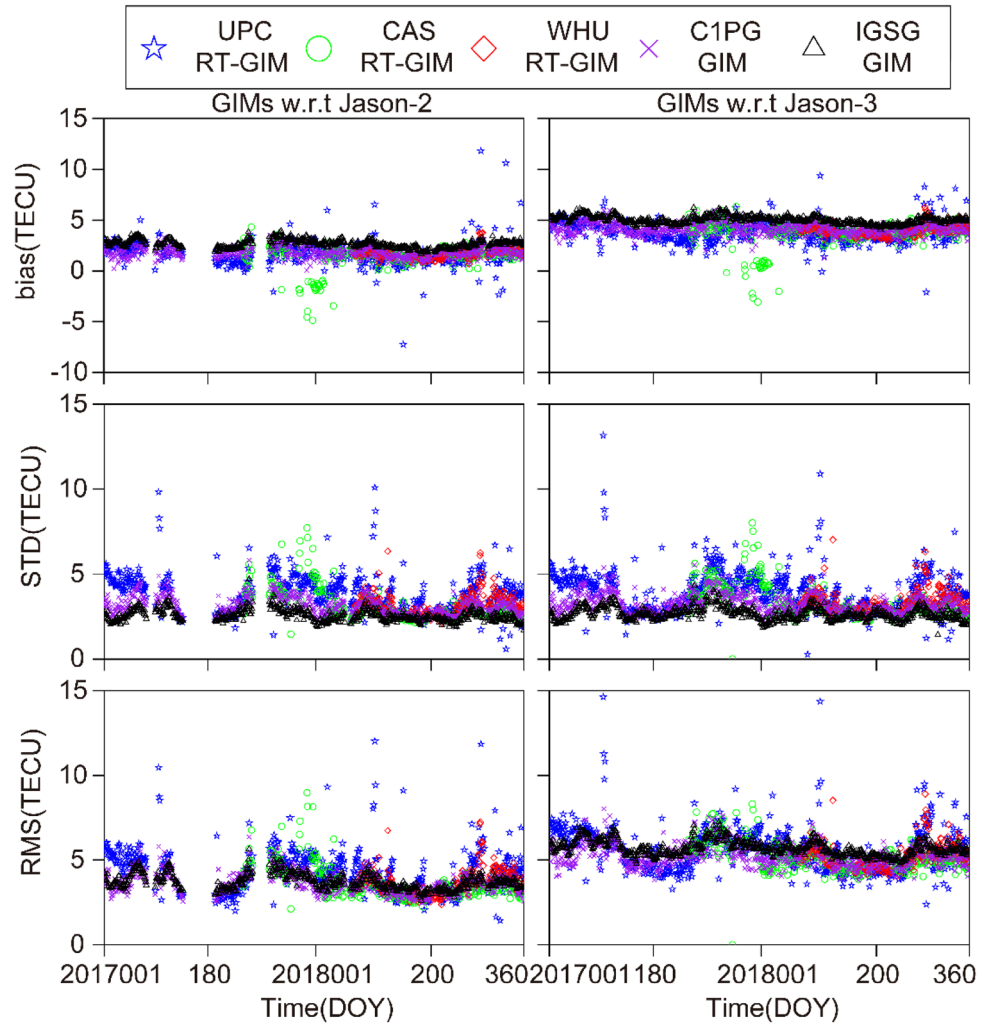

Table 4 Mean bias, STD, and RMS of the five GIMs relative to Jason VTEC during the experimental time period (without parentheses) and the common time period for the three RT-GIMs (with parentheses). Unit: TECU

IAACs	Bias	STD	RMS
Jason-2 VTEC			
UPC RT-GIM	1.79 (1.70)	3.96 (3.67)	4.44 (4.19)
CAS RT-GIM	1.55 (1.72)	3.05 (2.72)	3.59 (3.24)
WHU RT-GIM	1.77 (1.77)	3.25 (3.25)	3.71 (3.71)
C1PG GIM	1.82 (1.74)	3.12 (2.90)	3.64 (3.40)
IGSG GIM	2.68 (2.52)	2.54 (2.44)	3.70 (3.51)
Jason-3 VTEC			
UPC RT-GIM	4.00 (3.84)	4.94 (6.02)	5.71 (5.45)
CAS RT-GIM	3.88 (4.03)	3.24 (2.86)	5.21 (4.95)
WHU RT-GIM	4.04 (4.04)	3.38 (3.38)	5.28 (5.28)
C1PG GIM	4.15 (4.04)	3.24 (3.06)	5.28 (5.08)
IGSG GIM	5.04 (4.86)	2.65 (2.56)	5.70 (5.50)

available; the black squares indicate the value is larger than 15 TECU while the white parts mean that it is less than −15 TECU. As we can see, the biases of all GIMs relative to Jason-2/3 VTEC show a similar variation worldwide. The maximum values appear around the magnetic equator which is about 4 TECU for Jason-2 VTEC and about 6 TECU for Jason-3 VTEC. The positive biases denote the plasmaspheric electron content between the orbital altitude of GNSS satellites and that of Jason-2/3 satellites. Also, the bias over the ocean at high latitudes is smaller than the other regions.

To demonstrate the performance of the various RT-GIMs in the different latitude areas, we calculate the statistics shown in Fig. 10. As the figure shows, all GIMs have a typical U shape in terms of the geographic latitude except for UPC RT-GIM. In terms of UPC and WHU RT-GIM, they show a smaller value in the northern high-latitude area. However, CAS RT-GIM and C1PG GIM show a lower value in the north of the high-latitude area for Jason-2 data, while IGSG GIM is higher than Jason-2 at all latitudes. Also, all five GIMs have a higher bias at all latitudes for

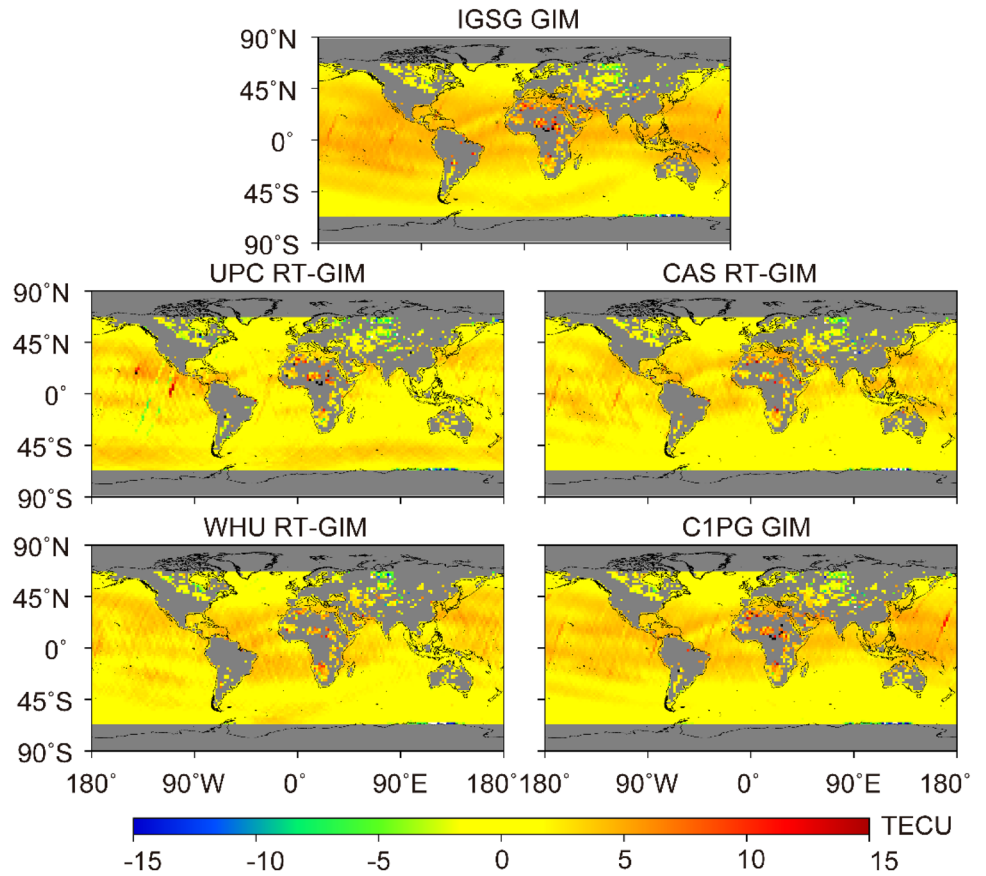**Fig. 8** Bias distribution of the differences between the five GIM products and Jason-2 VTEC data

Fig. 9 Bias distribution of the differences between the five GIM products and Jason-3 VTEC data
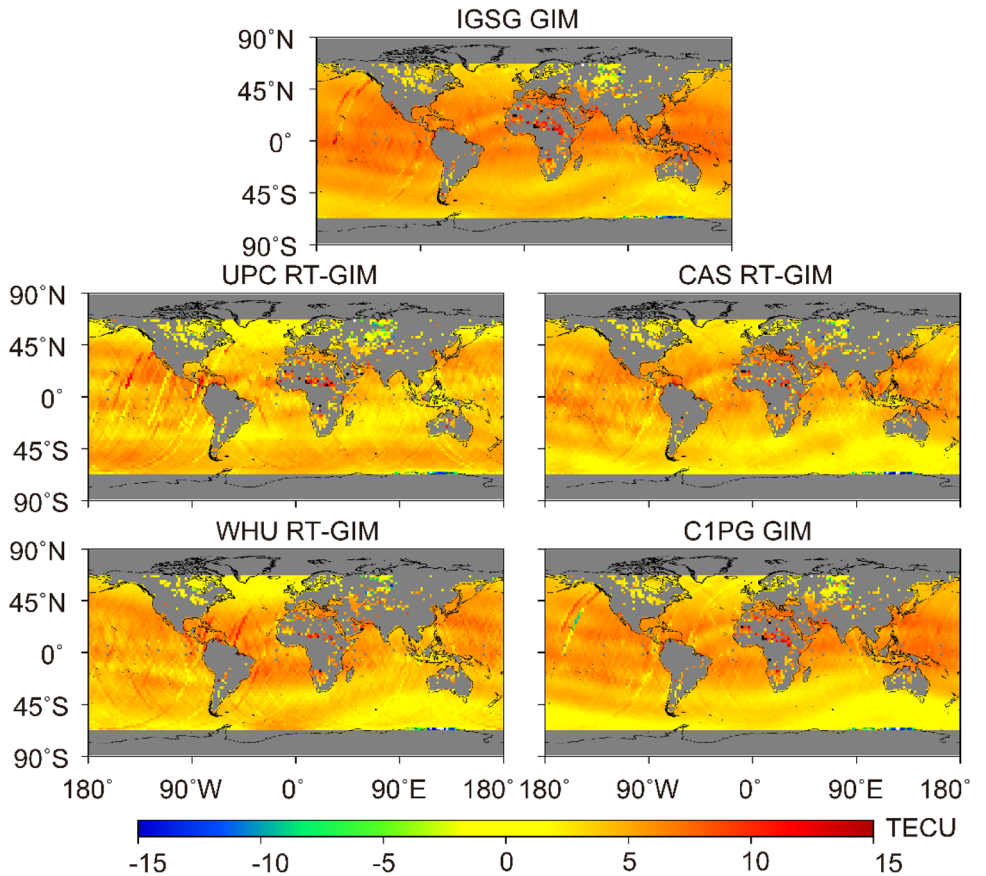
Fig. 10 Bias, STD, and RMS values of the differences between the five GIMs products and Jason-2/3 VTEC data
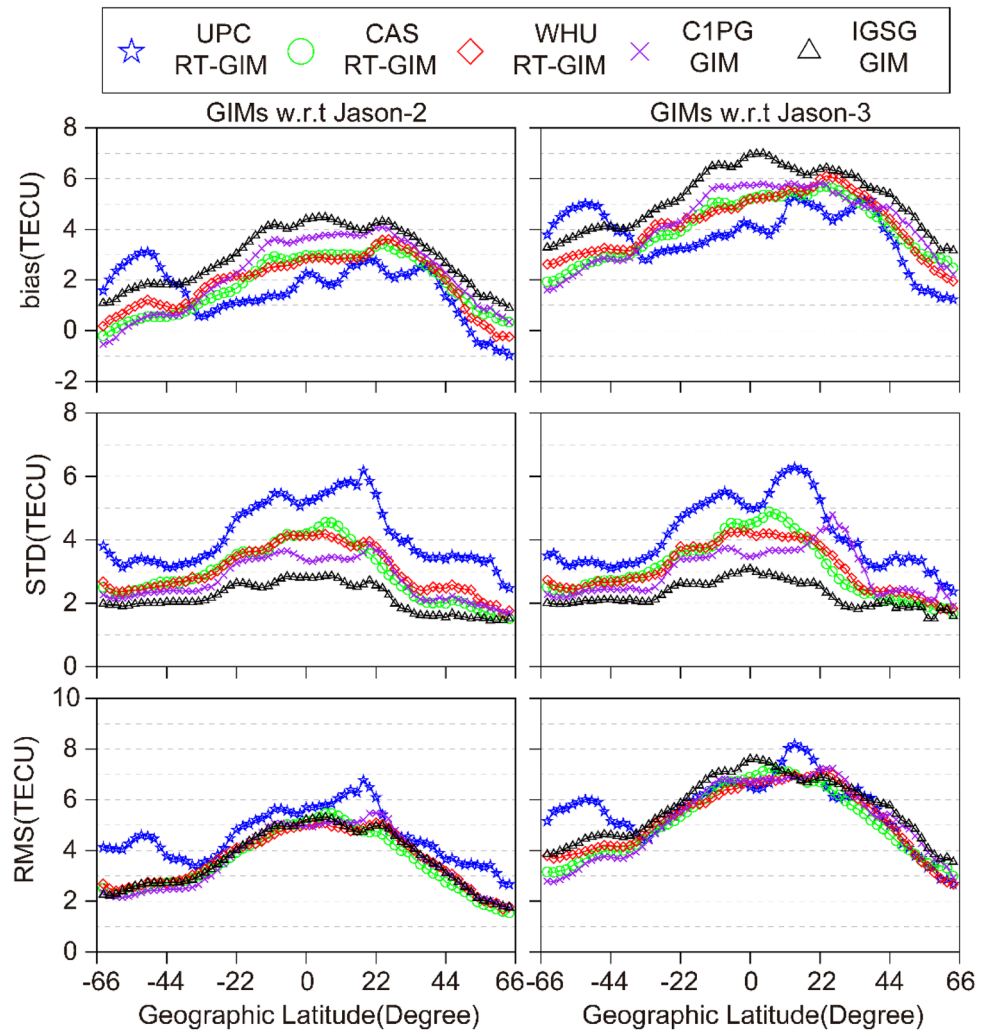

Fig. 11 Distribution of the validation stations, IGSG stations, C1PG stations, and RT-GIM station
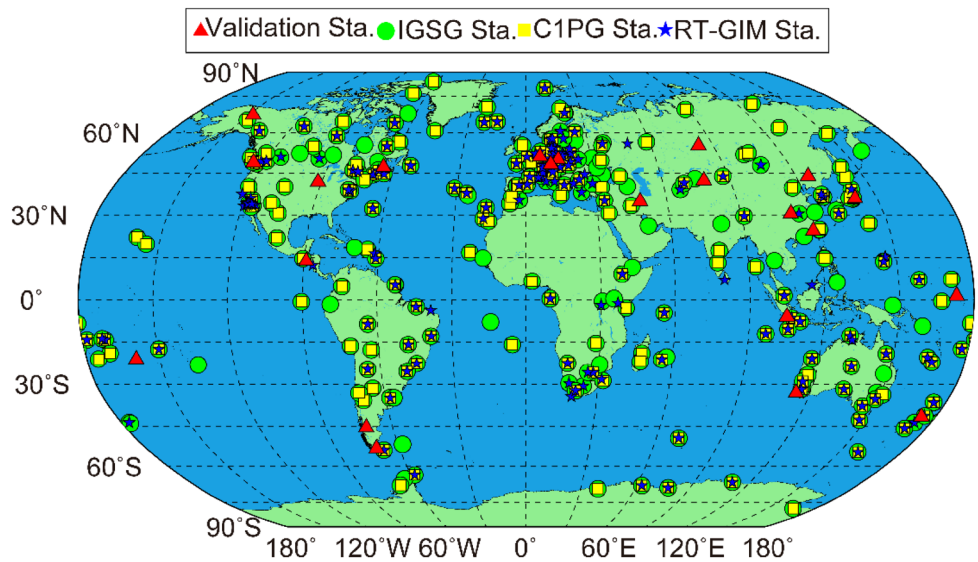
Fig. 12 Bias, STD, and RMS
values of five GIMs products
relative to the observed dSTEC
from DOY 001, 2017, to DOY
365, 2018
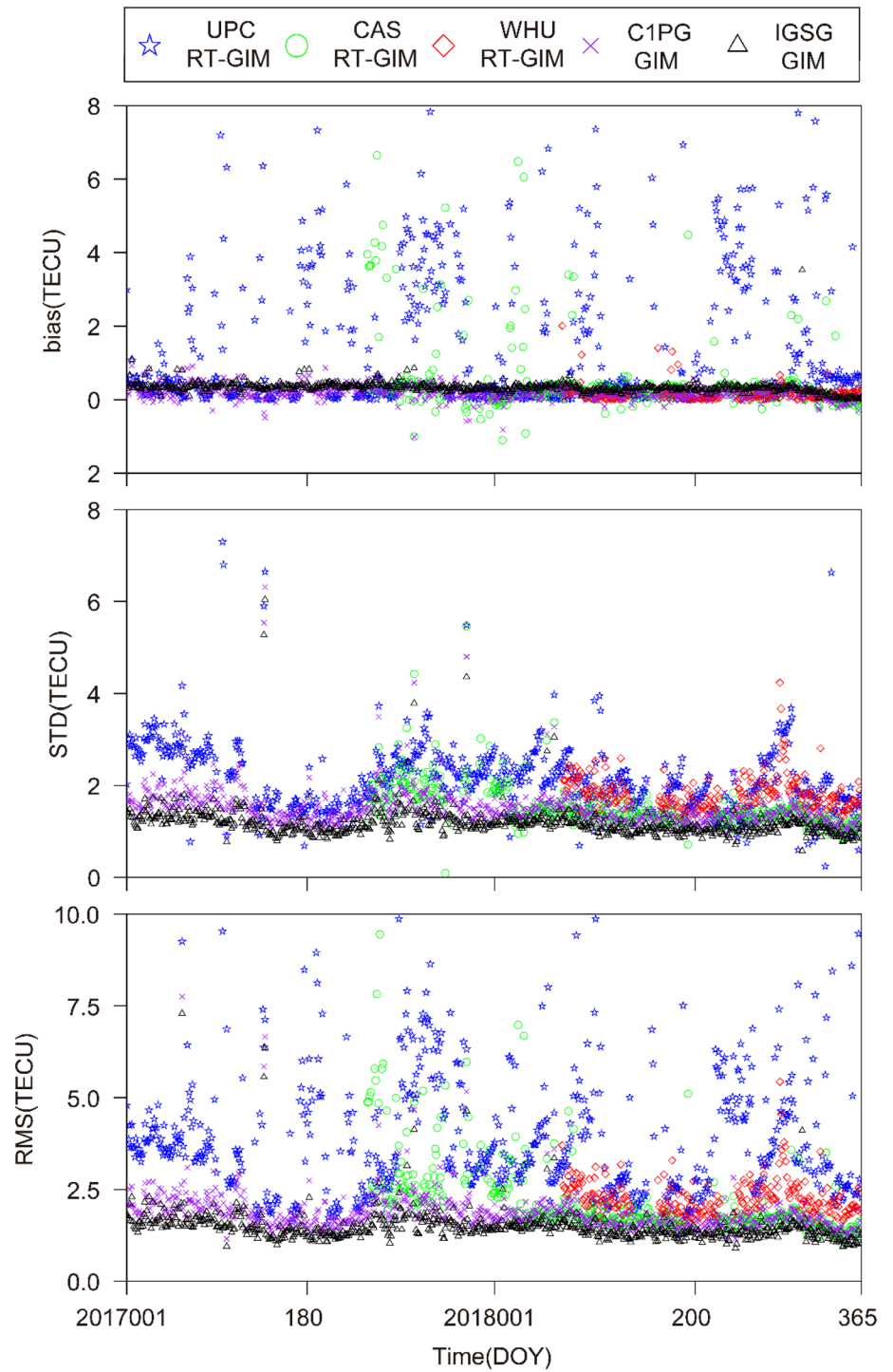
Table 5 Mean value of bias, STD, RMS of the five GIM products during the experimental time period (without parentheses) and the common
time period for the three RT-GIMs (with parentheses). Unit: TECU

Item	UPC RT-GIM	CAS RT-GIM	WHU RT-GIM	C1PG GIM	IGSG GIM
Bias	1.42 (1.54)	0.50 (0.28)	0.16 (0.16)	0.20 (0.15)	0.33 (0.28)
STD	2.24 (2.04)	1.51 (1.32)	1.84 (1.84)	1.52 (1.34)	1.19 (1.06)
RMS	4.02 (4.01)	2.16 (1.72)	2.29 (2.29)	1.86 (1.65)	1.49 (1.34)

Fig. 13 Histogram of daily mean bias, STD and RMS of the five GIM products for dSTEC from DOY 001, 2017, to DOY 365, 2018 for each available day
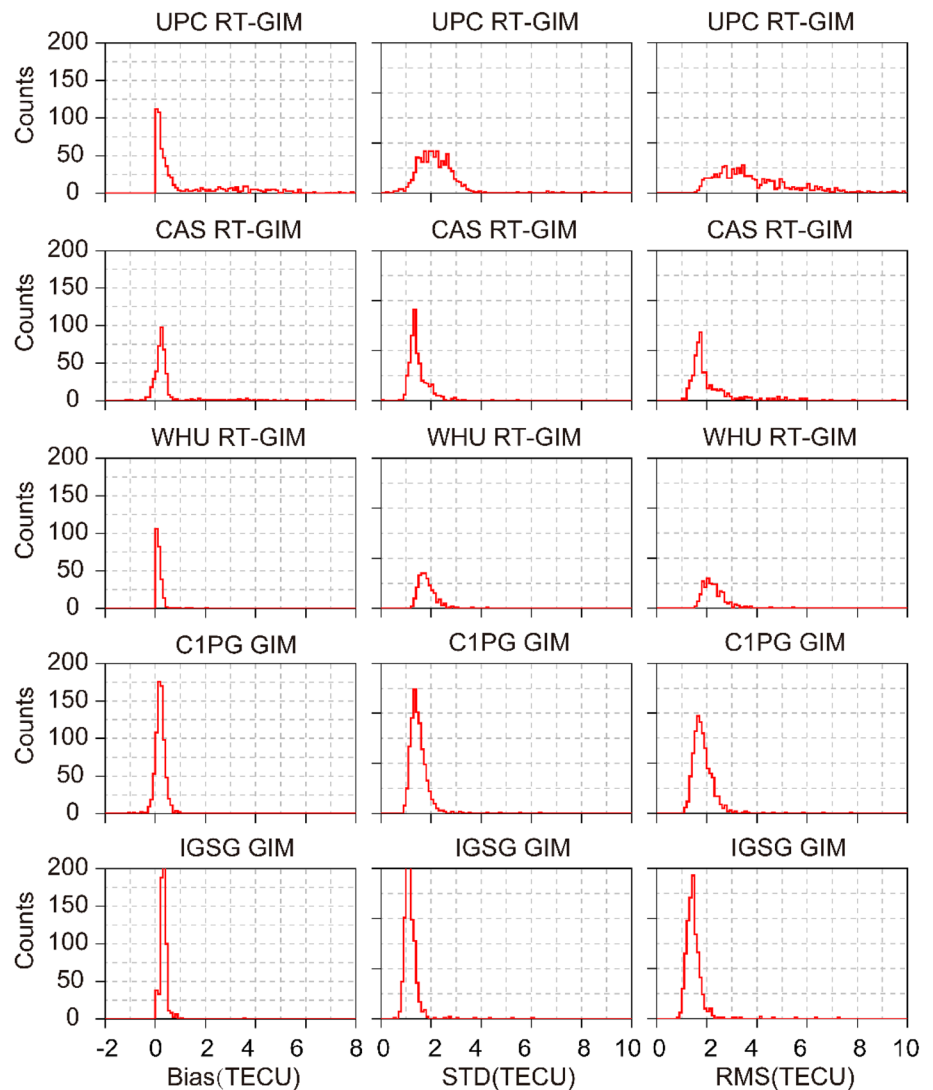
Jason-3 data while STD and RMS for different GIMs in the Southern Hemisphere are higher than that in the Northern Hemisphere, which is consistent with the smaller number of available receivers. The figure also shows that CAS and WHU RT-GIM perform a slightly worse than C1PG GIM, and C1PG GIM performs worse than IGSG GIM over the oceanic regions.

Validation against dSTEC and self-consistency analysis

To analyze the self-consistency of the five GIMs using dSTEC assessment method, a set of 55 IGS monitoring stations are selected to perform the test from DOY 001, 2017, to DOY 365, 2018. The distribution of the selected stations is shown in Fig. 11. The red triangles denote the validation stations which are not used when generating the IGSG GIM, C1PG GIM, and RT-GIMs; green circles are the stations

used to generate IGSG GIM; yellow squares express the stations used to obtain C1PG GIM; blue pentacles are the stations that can provide real-time stream data which may be used to obtain RT-GIMs for the three IAACs. As one can see, some validation stations are colocated with IGSG stations, C1PG stations, and RT-GIM stations. The selected stations are evenly distributed at high, middle, and low latitudes, which is helpful in demonstrating the accuracy and self-consistency of RT-GIMs as well as C1PG GIM and IGSG GIM.

The time series of bias, the STD and RMS of different GIMs products relative to the observed dSTEC are plotted in Fig. 12. It is shown that IGSG GIM is the best among these five GIMs, followed by C1PG GIM. The bias of IGSG GIM ranges from 0 to 0.5 TECU, while that of C1PG GIM is around 0 TECU. However, the STDs vary from 1.5 to 2.0 TECU for IGSG GIM and are about 2.0 TECU for C1PG GIM. The RMS for IGSG GIM is mostly about 1.5 TECU

Fig. 14 RMS values of the five GIMs for each station at different latitude compared with differences between the observation and computed dSTEC over the experimental period
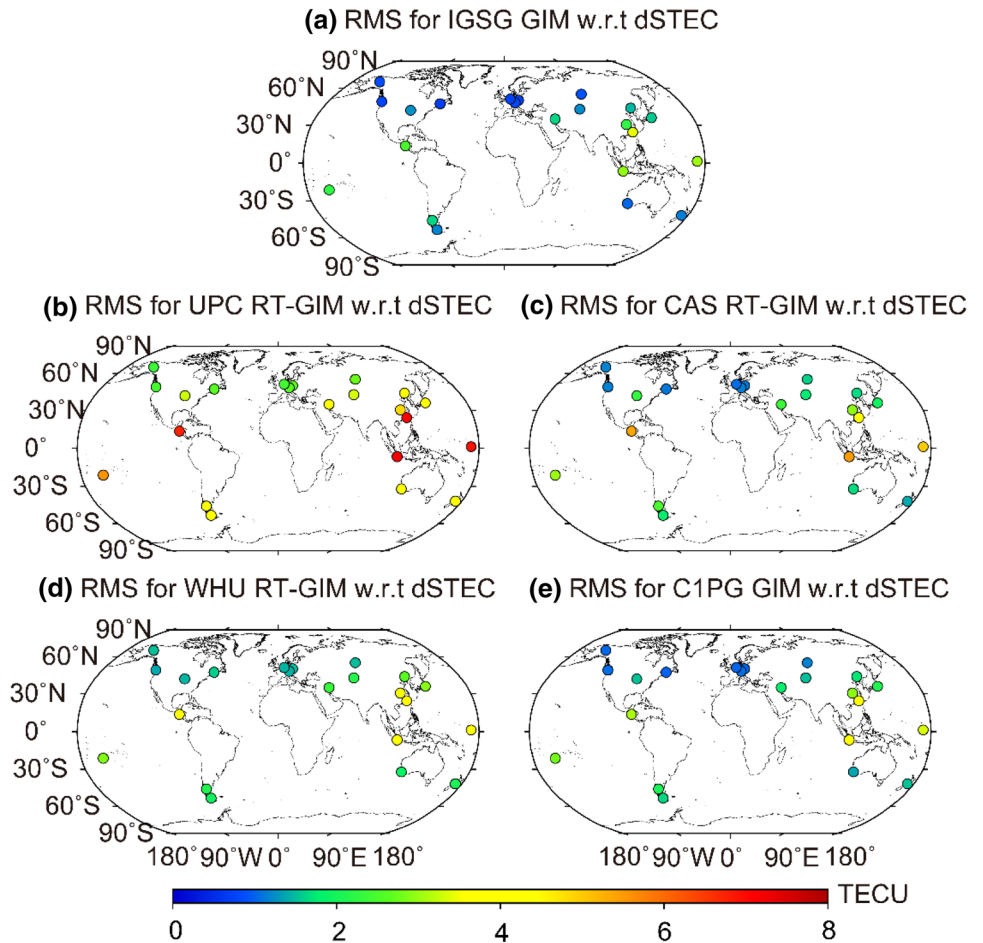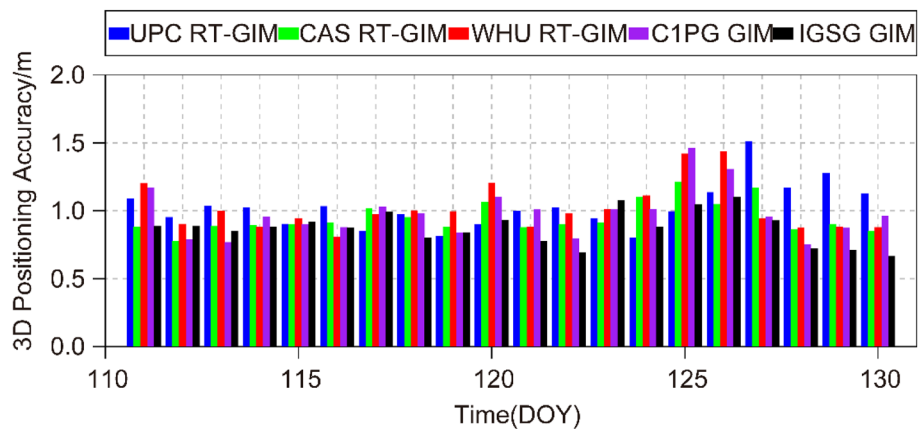

Fig. 15 Statistical results of 3D errors for different GIM products

and about 2.0 TECU for C1PG GIM. For RT-GIMs, the STD and RMS of CAS RT-GIM are smaller than the other two RT-GIMs after DOY 001, 2018, with values about 2.0 TECU for STD and about 2.5 TECU for RMS. In addition, there are some scatters for the three RT-GIMs, e.g., UPC RT-GIM has the most scatters, followed by CAS RT-GIM and WHU RT-GIM. It is noted that the STD and RMS values of UPC RT-GIM have a periodic divergence term while the

other two RT-GIMs do not. The reason could be related to a major problem with the update of the UPC predicted GIM needed for kriging interpolation (Hernández-Pajares 2019), coinciding with a worsening of URTG compared with previous assessments (Roma et al. 2016).

The mean values of bias, STD, and RMS for the five GIMs during the test period (without parentheses) and their common time period (with parentheses) are shown

Table 6 Mean positioning accuracy over 20 days of SF-PPP using the five GIM products. Unit: m

Products	North	East	Horizontal	Vertical
UPC RT-GIM	0.363	0.339	0.496	1.026
CAS RT-GIM	0.399	0.342	0.526	0.942
WHU RT-GIM	0.455	0.341	0.569	1.012
C1PG GIM	0.402	0.324	0.516	0.972
IGSG GIM	0.313	0.272	0.415	0.871

in Table 5. The table indicates that IGSG GIM is the best among the five GIMs followed by C1PG GIM; the RT-GIMs perform slightly worse than C1PG GIM. For the RT-GIMs, the performances of CAS RT-GIM and WHU RT-GIM are nearly the same. The series of bias, STD, and RMS are confirmed in the histograms shown in Fig. 13. It can be seen that the five GIMs have a similar trend with a fast decay of the counts. The bias, STD, and RMS of IGSG GIM performed best among the five GIMs, followed by C1PG GIM. The mean bias of UPC RT-GIM, CAS RT-GIM, and WHU RT-GIM range from 0 to 1.0, −0.3 to 0.8, and 0 to 0.5 TECU, respectively, while the corresponding RMS is 4.02, 2.16,

and 2.29 TECU during the test period, respectively. To study the latitude behavior of different GIMs with dSTEC assessment method for the entire test period, we plot the statistical results of the five GIMs for each station in Fig. 14. As we can see, the RT-GIMs perform slightly worse than C1PG GIM and IGSG GIM, especially in the equatorial ionization anomaly regions as well as oceanic islands.

Validation against SF-PPP solution

SF-PPP solution is carried out to investigate the quality of three RT-GIMs as well as C1PG GIM and IGSG GIM. The experiment uses GNSS data from DOY 111 to 130, 2018. The selected stations are the same as used in the dSTEC assessment method (Fig. 11), and the detailed SF-PPP processing strategies are introduced in Table 2.

The daily mean positioning accuracy corrected by different GIMs is presented in Fig. 15. The positioning result can reach meter level in 3D for all five GIMs generally. Among them, the positioning accuracy of SF-PPP corrected by RT-GIMs is slightly worse than that for C1PG GIM. Also, the post-processed IGSG GIM is the best among the five GIMs. Its maximum value is about (1.51, 1.21, 1.44, 1.46, 1.10) m

Fig. 16 3D positioning accuracy of SF-PPP with different GIMs for the test stations

(a) Positioning Accuracy of IGSG GIM

(b) Positioning Accuracy of UPC RT-GIM

(c) Positioning Accuracy of CAS RT-GIM

(d) Positioning Accuracy of WHU RT-GIM

(e) Positioning Accuracy of C1PG GIM
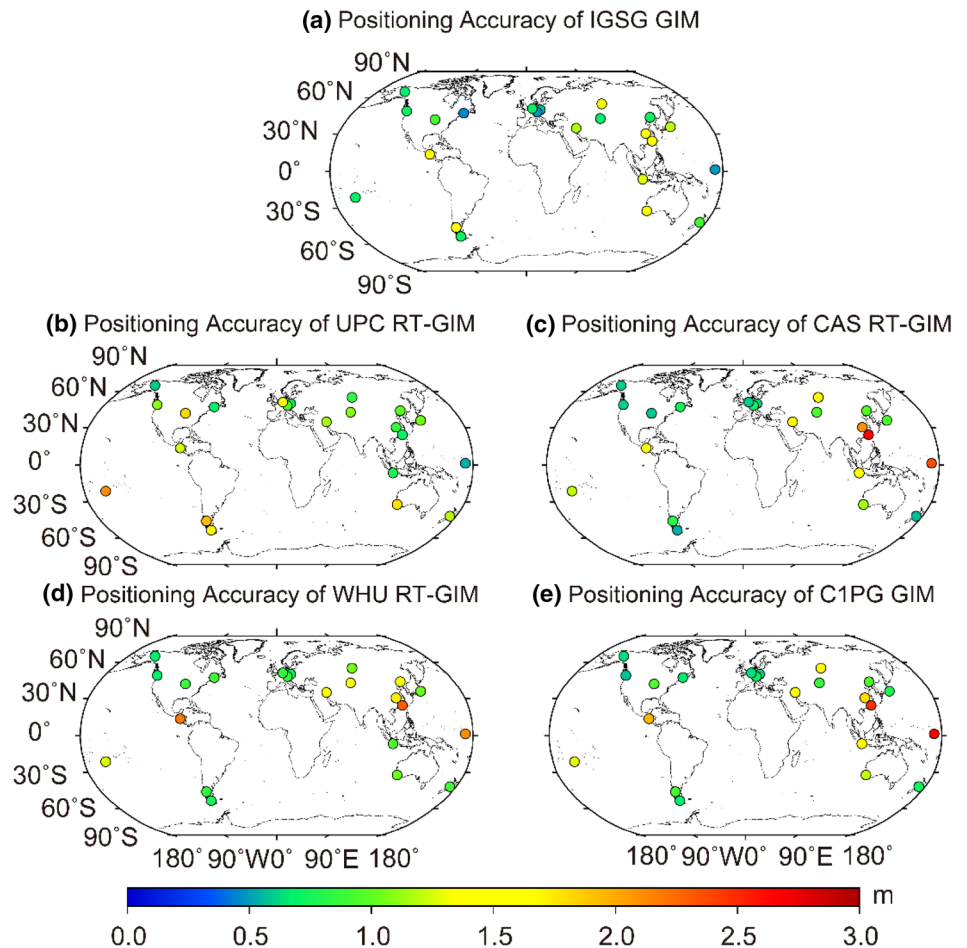
for (UPC RT-GIM, CAS RT-GIM, WHU RT-GIM, C1PG GIM, IGSG GIM). Moreover, the CAS RT-GIM performs more stable than the other two RT-GIMs. Table 6 lists the mean positioning accuracy using the different GIMs during the experimental period. The results show that the positioning accuracy can reach decimeter level in horizontal direction and meter level in the vertical direction. The performance of IGSG GIM is the best, followed by C1PG GIM and RT-GIMs. The CAS RT-GIM performs better than the other two RT-GIMs and C1PG GIM, with a positioning accuracy in horizontal and vertical directions of 0.526 and 0.942 m, respectively. However, UPC RT-GIM performs nearly the same as WHU RT-GIM.

The mean 3D positioning accuracy in 20 days at each station is plotted in Fig. 16. It shows that the positioning accuracy corrected by IGSG GIM is distinctly better than RT-GIMs and C1PG GIM in most areas. The performance of SF-PPP at the low latitude, where the ionosphere is very active, is worse than that in the other regions for all GIMs in general. It is noticeable; however, the current three RT-GIMs have a similar accuracy as IGSG GIM at mid and high latitudes and are also nearly the same as that with C1PG GIM.

Conclusions

In this study, we evaluated in detail the quality and performance of the current three real-time ionospheric products provided by the IAACs, i.e., UPC RT-GIM, CAS RT-GIM, and WHU RT-GIM). All available RT-GIMs from 2017 to 2018 are collected to be tested against with IGSG GIM, C1PG GIM, Jason-2/3 VTEC, and dSTEC truth data derived from 22 IGS global stations, which are not used to generate the RT-GIMs, C1PG GIM, and IGSG GIM. Moreover, the performance of SF-PPP in the position domain corrected by different ionospheric products is also carefully analyzed.

First, the comparison with IGSG GIM shows that the RT-GIMs perform nearly at the same level same as C1PG GIM. However, the UPC RT-GIM is not as good as the other two RT-GIMs. Its largest differences can reach up to 10–20 TECU in some regions. The mean differences for UPC RT-GIM, CAS RT-GIM, WHU RT-GIM, and C1PG GIM are about $-0.97, -0.90, -0.77$, and -0.80 TECU, respectively. Over the oceanic regions, the Jason-2/3 VTEC validation shows that the performance of the RT-GIMs is nearly the same as that of C1PG GIM. For the RT-GIMs, CAS RT-GIM and WHU RT-GIM match Jason-2/3 VTEC better than UPC RT-GIM.

The dSTEC derived from GNSS phase observations of 22 IGS stations, which might not be involved in the generation of the RT-GIMs, the C1PG GIM, and the IGSG GIM, are used to analyze the self-consistency of RT-GIMs with IGSG GIM and C1PG GIM from DOY 001, 2017, to DOY 365,

2018. The experiment results show that the mean RMS for UPC RT-GIM, CAS RT-GIM, and WHU RT-GIM is 4.02, 2.16, and 2.29, respectively, which is slightly worse than 1.86 TECU for C1PG GIM and 2.49 TECU for IGSG GIM. In general, the self-consistency of all tested GIMs is worse at low latitudes than the other regions.

Additionally, there is an interesting phenomenon that UPC RT-GIM, when it is provided in IONEX format, shows a periodic divergence term while the other two RT-GIMs do not. However, this is not the case when it is provided in spherical harmonic expansion and broadcast in RTCM format (Hernández-Pajares 2019). This different UPC RT-GIM behavior, especially the one given in IONEX format, is under investigation at UPC.

Finally, an SF-PPP experiment is performed based on the selected stations during 20 days to further assess the quality of RT-GIMs and C1PG GIM as well as IGSG GIM in positioning domain. The positioning accuracy using RT-GIMs can reach decimeter level in the horizontal direction and meter level in the vertical direction, which is nearly the same obtained with C1PG GIM and slightly worse than with IGSG GIM. The worst 3D positioning accuracy is about (1.51, 1.21, 1.44, 1.46, 1.10) m for (UPC RT-GIM, CAS RT-GIM, WHU RT-GIM, C1PG GIM, IGSG GIM). The positioning performance for the stations located at the low latitude is higher than for stations located in the other areas. It should be noted that, since the stations selected for the validation using dSTEC method and SF-PPP method may be included by the IAAC for RT-GIM calculation, this study may overestimate the performance of RT-GIM.

References

Angrisano A, Gaglione S, Gioia C, Massaro M, Robustelli U (2013) Assessment of NeQuick ionospheric model for Galileo single-frequency users. Acta Geophys 61(6):1457–1476

Bi T, An J, Yang J, Liu S (2017) A modified Klobuchar model for single-frequency GNSS users over the polar region. Adv Space Res 59(3):833–842

Brunini C, Azpilicueta F (2010) GPS slant total electron content accuracy using the single layer model under different geomagnetic regions and ionospheric conditions. J Geod 84(5):293–304

Brunini C, Azpilicueta F, Gende M, Camilion E, Ángel AA, Hernández-Pajares M, Juan M, Sanz J, Salazar D (2011a) Ground- and space-based GPS data ingestion into the NeQuick model. J Geod 85(12):931–939

Brunini C, Camilion E, Azpilicueta F (2011b) Simulation study of the influence of the ionospheric layer height in the thin layer ionospheric model. J Geod 85(9):637–645

Chen J, Huang L, Liu L, Wu P, Qin X (2017) Applicability analysis of VTEC derived from the sophisticated Klobuchar model in China. ISPRS Int J Geo-Inf 6(3):75

Choy S (2009) An investigation into the accuracy of single frequency precise point positioning (PPP). Ph.D. thesis, RMIT University, Australia

Ciraolo L, Azpilicueta F, Brunini C, Meza A, Radicella SM (2007) Calibration errors on experimental slant total electron content (TEC) determined with GPS. J Geod 81(2):111–120

Davies K (1990) Ionospheric radio. Peter Perrgrinus Ltd., London

Feltens J (2003) The activities of the Ionosphere working group of the International GPS Service (IGS). GPS Solut 7(1):41–46

Feltens J, Angling M, Jackson-Booth N, Jakowski N, Hoque M, Hernández-Pajares M, Aragón-Àngel A, Orús R, Zandbergen R (2011) Comparative testing of four ionospheric models driven with GPS measurements. Radio Sci 46(6):RS0D12

García-Rigo A, Monte E, Hernández-Pajares M, Juan JM, Sanz J, Aragón-Angel A, Salazar D (2011) Global prediction of the vertical total electron content of the ionosphere based on GPS data. Radio Sci 46(6):RS0D25

Hadas T, Bosy J (2015) IGS RTS precise orbits and clocks verification and quality degradation over time. GPS Solut 19(1):93–105

Hernández-Pajares, M. et al. (2019) Recent UPC-IonSAT results on global RT and other ionospheric modelling problems. Presentation at the 10th China satellite navigation conference (CSNC2019), Beijing, May 2019

Hernández-Pajares M, Juan JM, Sanz J, Orús R, Garcia-Rigo A, Feltens J, Komjathy A, Schaer SC, Krankowski A (2009) The IGS VTEC maps: a reliable source of ionospheric information since 1998. J Geod 83(3–4):263–275

Hernández-Pajares M, Roma-Dollase D, Krankowski A, García-Rigo A, Orús-Pérez R (2017) Methodology and consistency of slant and vertical assessments for ionospheric electron content models. J Geod 91(12):1405–1414

Hoque MM, Jakowski N (2015) An alternative ionospheric correction model for global navigation satellite systems. J Geod 89(4):391–406

Hoque MM, Jakowski N (2018) Berdermann J (2018) Positioning performance of the NTCM model driven by GPS Klobuchar model parameters. J Space Weather Space Clim 8:A20

Imel DA (1994) Evaluation of the TOPEX/POSEIDON dual-frequency ionosphere correction. J Geophys Res: Oceans 99(C12):24895–24906

Jee G, Lee HB, Kim YH, Chung JK, Cho J (2010) Assessment of GPS global ionosphere maps (GIM) by comparison between CODE GIM and TOPEX/Jason TEC data: ionospheric perspective. J Geophys Res Space Phys 115(A10):319

Kazmierski K, Sośnica K, Hadas T (2017) Quality assessment of multi-GNSS orbits and clocks for real-time precise point positioning. GPS Solut 22(1):11

Keshin M (2012) A new algorithm for single receiver DCB estimation using IGS TEC maps. GPS Solut 16(3):283–292

Klobuchar JA (1987) Ionospheric time-delay algorithm for single-frequency GPS users. IEEE Trans Aerosp Electron Syst 23(3):325–332

Komjathy A (1997) Global ionospheric total electron content mapping using the global positioning system. Ph.D. dissertation, Department of Geodesy and Geomatics Engineering, Technical report no. 188, University of New Brunswick, Fredericton, Canada

Li M, Yuan Y, Wang N, Li Z, Huo X (2018a) Performance of various predicted GNSS global ionospheric maps relative to GPS and JASON TEC data. GPS Solut 22:55

Li X, Xie W, Huang J, Ma T, Zhang X, Yuan Y (2018b) Estimation and analysis of differential code biases for BDS3/BDS2 using iGMAS and MGEX observations. J Geod 93(3):419–435

Mannucci AJ, Wilson BD, Yuan DN, Ho CH, Lindqwister UJ, Runge TF (1998) A global mapping technique for GPS-derived ionospheric total electron content measurements. Radio Sci 33(3):565–582

Nava B, Coïsson P, Radicella SM (2008) A new version of the NeQuick ionosphere electron density model. J Atmos Terr Phys 70(15):1856–1862

Nie Z, Yang H, Zhou P, Gao Y, Wang Z (2019) Quality assessment of CNES real-time ionospheric products. GPS Solut 23:11

Orús R, Hernández-Pajares M, Juan JM, Sanz J, García-Fernández M (2002) Performance of different TEC models to provide GPS ionospheric corrections. J Atmos Terr Phys 64(18):2055–2062

Orús R, Hernández-Pajares M, Juan J, Sanz J (2005) Improvement of global ionospheric VTEC maps by using kriging interpolation technique. J Atmos Solar-Terr Phys 67(16):1598–1609

Ren X, Zhang X, Xie W, Zhang K, Yuan Y, Li X (2016) Global ionospheric modelling using multi-GNSS: BeiDou, Galileo, GLONASS and GPS. Sci Rep 6:33499

Roma D, Hernandez M, Garcia-Rigo A, Laurichesse D, Schmidt M, Erdogan E, Yuan Y, Li Z, Gómez-Cama JM, Krankowski A (2016) Real time global ionospheric maps: a low latency alternative to traditional GIMs. In: 19th International Beacon satellite symposium (BSS 2016), Trieste, Italy, June 27–July 1, p 1

Roma-Dollase D, Hernández-Pajares M, Krankowski A, Kotulak K, Ghoddousi-Fard R et al (2018) Consistency of seven different GNSS global ionospheric mapping techniques during one solar cycle. J Geod 92(6):691–706

Schaer S (1999) Mapping and predicting the earth's ionosphere using the global positioning system. Ph.D. thesis, Institut für Geodäsie und Photogrammetrie, Eidg. Technische Hochschule Zürich

Schaer S, Gurtner W, Feltens J (1998) IONEX: the ionosphere map exchange format version 1. In: Proceedings of the IGS AC workshop, Darmstadt, Germany, vol 9

Wang N, Yuan Y, Li Z, Montenbruck O, Tan B (2016) Determination of differential code biases with multi-GNSS observations. J Geod 90(3):209–228

Wang N, Li Z, Min L, Yuan Y, Huo X (2018) GPS, BDS and Galileo ionospheric correction models: an evaluation in range delay and position domain. J Atmos Terr Phys 180:83–91

Wang N, Li Z, Yuan Y, Li M, Huo X, Yuan C (2019) Ionospheric correction using GPS Klobuchar coefficients with an empirical night-time delay model. Adv Space Res 63(2):886–896

Yuan Y, Huo X, Ou J, Zhang K, Chai Y, Wen D, Grenfell R (2008) Refining the Klobuchar ionospheric coefficients based on GPS observations. IEEE Trans Aero Electron Syst 44(4):1498–1510

Yunbin Y, Ningbo W, Zishen L, Xingliang H (2019) The BeiDou global broadcast ionospheric delay correction model (BDGIM)

and its preliminary performance evaluation results. Navigation 66(1):55–69

Yunck TP (1993) Coping with the atmosphere and ionosphere in precise satellite and ground positioning, Washington DC. Am Geophys Union Geophys Monogr Ser 73:1–16

Zhang X, Ma F, Ren X, Xie W, Zhu F, Li X (2017) Evaluation of NTCM-BC and a proposed modification for single-frequency positioning. GPS Solut 21(4):1535–1548

Zhang L, Yang H, Gao Y, Yao Y, Xu C (2018) Evaluation and analysis of real-time precise orbits and clocks products from different IGS analysis centers. Adv Space Res 61(12):2942–2954

Publisher's Note Springer Nature remains neutral with regard to jurisdictional claims in published maps and institutional affiliations.

Xiaohong Zhang is currently a professor at Wuhan University. He obtained his B.Sc., Master, and Ph.D. degrees with distinction in Geodesy and Engineering Surveying at the School of Geodesy and Geomatics in Wuhan University in 1997, 1999, and 2002. His main research interests include precise point positioning and GNSS/INS.

Xiaodong Ren is postdoctoral researcher at Wuhan University. He obtained his B.Sc., Master, and Ph.D. degrees with distinction in Geodesy and Engineering Surveying at the School of Geodesy and Geomatics in Wuhan University in 2011, 2013, and 2017. His main research focuses on PPP-RTK and ionospheric modeling.

Mohamed Freeshah is currently a Ph.D. scholar at State Key Laboratory of Information Engineering in Surveying, Mapping and Remote Sensing, Wuhan University. He received Bachelor and M.Sc. in Geodesy and Surveying from Benha University in 2010 and 2016, respectively. He has worked as a teaching assistant from 2011 to 2016. His main research interests include GNSS and ionospheric disturbances.

Jun Chen is currently a Ph.D. candidate at the Wuhan University. He obtained his Master degrees in College of Geomatics and Geoinformation in the Guilin University of Technology. His main research focuses on ionospheric modeling and monitoring.
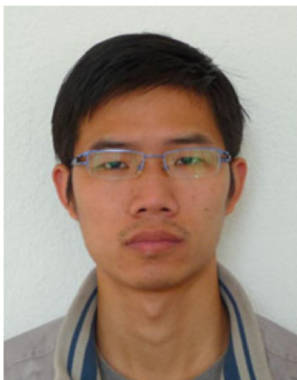
Xingxing Li received his Ph.D. student at the Department of Geodesy and Remote Sensing of the German Research Centre for Geosciences (GFZ). He holds a B.S. degree in Geodesy and Geomatics from Wuhan University in China. His current research focuses on the development of real-time GNSS precise positioning techniques.